HNUE JOURNAL OF SCIENCE
Natural Sciences 2025, Volume 70, Issue 4, pp. 78-87
This paper is available online at http://hnuejs.edu.vn/ns
DOI: 10.18173/2354-1059.2025-0056

CHARACTERIZATION OF A CHITOSAN/POLYANILINE FILM LOADED WITH LOVASTATIN

Bui Thanh Nga[1], Huynh Xuan Mai[1], Vu Quoc Manh[2],
Nguyen Dang Dat[1], Vu Thi Huong[1] and Vu Quoc Trung[1,*]
[1]*Faculty of Chemistry, Hanoi National University of Education, Hanoi city, Vietnam*
[2]*Institute of Medicine and Pharmacy, Thanh Do University, Hanoi city, Vietnam*
[*]Corresponding author: Vu Quoc Trung, e-mail: trungvq@hnue.edu.vn

Received September 26, 2025. Revised November 27, 2025. Accepted December 30, 2025.

Abstract. This research aims to address these challenges by dispersing the drug within both a single biopolymer matrix (chitosan) and a dual biopolymer matrix (chitosan/polyaniline). The results indicated that, among the single-matrix chitosan/lovastatin (CsL) samples, the CsL10 CsL10 exhibits the most favorable drug-release behavior over 30 h, achieving a cumulative release of 96% in simulated intestinal fluid (pH 7.4) while providing effective drug protection of 10.5% in simulated gastric fluid (pH 2.0). These findings suggest a promising platform for further development. Building upon this direction, the study was extended to incorporate polyaniline to enable live-function monitoring and tissue stimulation. The results showed that the chitosan/polyaniline/lovastatin (CsPL) samples met the initial expectations, with the CsPL7 sample exhibiting drug release rates of 92.23% and 18.58% in the simulated intestinal and gastric environments, respectively. Analytical techniques, including FT-IR, FESEM, DSC, and UV-Vis, were employed to gain a deeper understanding of the interactions between the polymer components and the drug substance.

Keywords: chitosan/PANi/lovastatin biocomposites, chitosan/lovastatin biocomposites, lovastatin release, polyaniline.

1. Introduction

Lovastatin (Lov), a leading cholesterol-lowering drug, functions by competitively inhibiting HMG-CoA reductase [1], [2]. However, its clinical utility is hampered by poor aqueous solubility (~0.4×10^{-3} mg/mL), low oral bioavailability (< 5%), and a short half-life (1- 2 h) [3]. Advanced drug delivery systems based on polymeric composites present a viable strategy to overcome these limitations by enhancing solubility and enabling controlled release.

Polymer composites demonstrate remarkable versatility. Chitosan, for instance, has been utilized in hemostatic materials [4] and food preservation nanocomposites [5]. Critically, within drug delivery, the composition of the polymer matrix is paramount, as evidenced by chitosan/carrageenan blends where the biopolymer ratio directly governed lovastatin release [6]. This underscores the potential of composite design for tailored drug delivery.

A significant trend involves integrating functional synthetic polymers with natural biopolymers to create intelligent, multi-responsive systems. pH-responsive carriers, for example, can target specific sites like the gastrointestinal tract [7]. The conducting polymer polyaniline (PANi) is particularly promising due to its electrical conductivity and tunable biocompatibility [8]. PANi has been successfully incorporated into various drug carriers [9]-[12] and sophisticated hybrids like magnetic GO-Fe_3O_4-PANi nanoparticles for cancer therapy [13]. The synergy between chitosan and PANi has also been explored for pH-dependent release [14], aligning with the broader development of multi-functional biomaterials [15].

Despite these advancements, chitosan/polyaniline composites specifically designed for lovastatin delivery remain unexplored. Although the influence of polymer ratios in binary systems has been reported [6], a systematic investigation of lovastatin-loaded chitosan (CsLov) with varying drug contents and, more importantly, of novel chitosan/polyaniline (CsPLov) biocomposites has not been conducted yet. This study therefore aims to: (i) synthesize and characterize CsLov (3-15% Lov) and CsPLov (0-10% PANi) composites; (ii) evaluate their drug release profiles in simulated gastric (pH 2.0) and intestinal (pH 7.4) fluids; and (iii) assess the impact of PANi content on Lov release kinetics.

2. Content

2.1. Chemicals and experimental methods

**** Chemicals***

Lov (≥ 98%) was purchased from Rhawn (China); Chitosan powder (purity ≥ 95) and aniline in liquid form were bought from Aladdin Co, China. Other chemicals, such as acetic acid, ethanol, hydrochloric acid, potassium chloride, sodium hydroxide, and potassium dihydrogen phosphate, were of analytical or reagent grade and used as received.

**** Synthesis of Lov-carrying chitosan biocomposites with variable content of Lov***

Table 1. Symbols and compositions of the CsL composite samples

No.	Symbols of the samples	Cs (g)	Lov (g)
1	CsL3	1.0	0.03
2	CsL5	1.0	0.05
3	CsL7	1.0	0.07
4	CsL10	1.0	0.10
5	CsL15	1.0	0.15

Lovastatin-loaded chitosan (CsLov) composites were synthesized via solution casting. Chitosan (1 g) was dissolved in 1200 mL of 1% acetic acid at 30 °C to form solution A. A predetermined Lov amount was dissolved in ethanol (solution B). Solution B was added dropwise (3 mL/min) into solution A under homogenization (20,000 rpm). The resulting mixture was stirred magnetically (400 rpm, 1.5 h), casted into Petri dishes, and dried for 48 hours. The entire procedure was repeated in triplicate, and the results are presented as the mean value [6]. The symbols and compositions of the CsL composite samples in Table 1.

**** Synthesis of Lov-carrying chitosan/PANi biocomposites with variable content of PANi***

The Cs/PANi/Lov composite was fabricated by first dissolving chitosan (Cs, 1 g) in 1200 mL of 1% acetic acid at 30°C (mixture A). Aniline was then added and stirred for 20 minutes, followed by APS addition (1:1 molar ratio to aniline) with stirring for 1 hour to form mixture B. Mixtures A and B were combined to yield mixture C. Separately, lovastatin (Lov) was dissolved in ethanol (mixture D). Mixture D was added dropwise into mixture C under high-speed homogenization (20,000 rpm, 5 min) to form mixture E, which was then magnetically stirred (400 rpm, 1.5 h). The final mixture was casted into a Petri dish and dried under ambient conditions for 48 hours. The entire procedure was repeated in triplicate, and the results are presented as the mean value [6]. The symbols and compositions of the CsPL composite samples are shown in Table 2.

Table 2. Symbols and compositions of the CsPL composite samples

No.	Symbols of the samples	Cs (g)	Lov (g)	Aniline (mL)	APS (g)
1	CsPL0	1.0	0.10	0.00	0.000
2	CsPL3	1.0	0.10	0.03	0.075
3	CsPL5	1.0	0.10	0.05	0.125
4	CsPL7	1.0	0.10	0.07	0.175
5	CsPL10	1.0	0.10	0.10	0.250

**** Characterization of the CsCLP biocomposites***

FT-IR spectroscopy (Nexus 670) analyzed functional groups from 400 - 4000 cm^{-1}. UV-Vis spectroscopy (UV-1900) quantified drug release via calibration curves (200 - 400 nm). SEM (Hitachi S-4800) characterized the morphology after platinum coating. DSC (DSC60) determined thermal properties under nitrogen with a 10 °C/min ramp to 300 °C. Data processing utilized Microsoft Excel.

**** Study of drug release***

The *in vitro* release of lovastatin from CsL and CsPL composites was evaluated in simulated gastric (pH 2.0) and intestinal (pH 7.4) fluids at 37.0 ± 0.1 °C. A predetermined composite mass was immersed in 200 mL of buffer under constant agitation. Aliquots (5 mL) were sampled hourly, with fresh buffer replenished to maintain sink conditions. The absorbance values were converted to concentration using pre-established calibration curves for Lov in pH 2.0 ($y = 2598.2x - 0.1468$, $R^2 = 0.9972$) and pH 7.4 ($y = 3978x - 0.1975$, $R^2 = 0.9985$) buffers. All release studies were performed in triplicate to ensure data reliability.

2.2. Results and discussion

2.2.1. FT-IR spectrum of the lovastatin-loaded composites

2.2.1.1. FTIR spectra of CsL

FT-IR analysis (Figure 1) confirmed the structural integrity of lovastatin (Lov) within the CsL composites. The spectrum of pure Lov displayed characteristic bands: O-H stretch at 3544 cm^{-1}; C-H stretches (2965, 2929, 2807 cm^{-1}) for $-CH_3$, $-CH_2$, and -CH groups; and key functional group vibrations at 1700 cm^{-1}, 1726 cm^{-1} (C=O), and 1074 cm^{-1} (C-O-C) [16]. In the CsL composites, all characteristic peaks of both Cs and Lov remained present but exhibited slight shifts to lower wavenumbers [16]-[18]. Notably, the broad -OH/-NH stretch shifted to 2500 - 3500 cm^{-1}, and the C-O stretch to 1000 - 1300 cm^{-1}. These shifts are attributed to van der Waals interactions and hydrogen bonding between chitosan's $-NH_2$ groups and Lov's -C=O groups upon incorporation into the matrix [14]. The absence of new peaks or disappearance of key bands confirms that these are physical interactions, preserving the chemical integrity of both components. This demonstrates that the CsL system successfully maintains Lov's pharmaceutical activity.

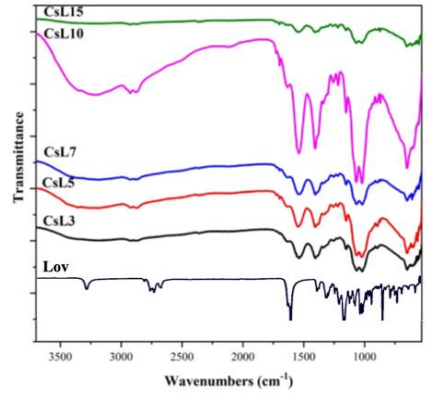

Figure 1. FTIR spectra of Lov and CsL composites

2.2.1.2. FT-IR spectra of CsPL

FT-IR analysis (Figure 2) confirmed the successful formation of CsPL composites through physical interactions. The spectrum of pure lovastatin (Lov) showed characteristic bands: a broad O-H stretch at 3544 cm^{-1}; C-H stretches at 2965, 2929, and 2807 cm^{-1} for $-CH_3$, $-CH_2$, and -CH groups; and key vibrations at 1700 cm^{-1}, 1726 cm^{-1} (C=O), and 1074 cm^{-1} (C-O-C) [20]. The PANi spectrum displayed its distinctive features: benzenoid and quinonoid ring stretches at 1560 cm^{-1} and 1483 cm^{-1}, respectively; N-H stretch at 3436 cm^{-1}; and other characteristic peaks at 1294 cm^{-1} (N=quinoid=N), 1240 cm^{-1} (C-N in aromatic ring), and 1097 cm^{-1} ($C–N^+$) [19]. Critically, all characteristic peaks of Cs, Lov, and PANi remained present in the composite spectra. However, they exhibited minor shifts, generally to lower wavenumbers. For instance, the broad -OH/-NH stretch appeared within 2920–3300 cm^{-1} and the C-O stretch between 1000–1300 cm^{-1}. These spectral changes are attributed to molecular interactions upon incorporating Lov into the chitosan-polyaniline matrix, specifically van der Waals forces and hydrogen bonding between chitosan's $-NH_2$ groups and Lov's -C=O groups [14]. The absence of any new peaks or disappearance of fundamental functional group vibrations confirms that no chemical reactions occurred.

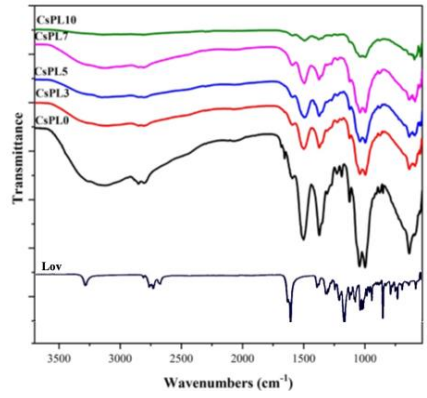

Figure 2. FTIR spectra of Lov and CsPL composites

Only physical interactions are formed, which preserve the chemical integrity and, consequently, the pharmaceutical activity of Lov within the CsPL drug carrier system.

2.2.2. Morphology of the lovastatin-loaded composites

2.2.2.1. Morphology of CsL composites

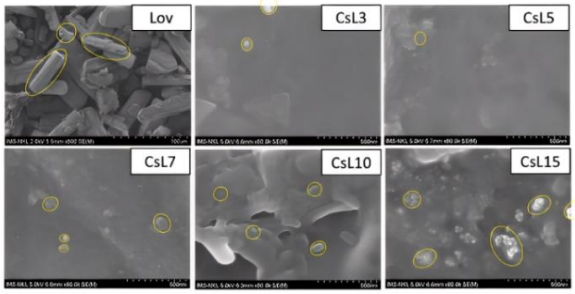

Figure 3. FESEM images of CsL composites with variable Lov contents

FESEM analysis (Figure 3) reveals a significant morphological transformation of lovastatin (Lov) within the CsL composites. Pure Lov exists as large, rod-like crystals (10-60 μm) [6], whereas within the chitosan (Cs) matrix, the drug adopts a spherical morphology with drastically reduced particle sizes (0.03 - 0.3 μm). This change and enhanced dispersion are attributed to hydrogen bonding between chitosan's -NH_2 groups and Lov's -OH groups, promoting integration into the polymer network. The dispersion uniformity was highly dependent on drug loading. The CsL10 sample exhibited optimal, uniform dispersion with particle sizes of 0.05–0.09 μm. In contrast, lower loadings (CsL3, CsL7) showed uneven distribution, potentially due to insufficient porosity, while the highest loading (CsL15) led to aggregation into larger clusters (0.1 - 0.3 μm). This aggregation at high concentration is likely caused by spatial hindrance, which limits the availability of binding sites and reduces hydrogen bonding efficiency. Despite this, the particle size in all composites remained substantially smaller than pure Lov, confirming the matrix's role in controlling morphology and size through intermolecular interactions.

2.2.2.2. Morphology of CsPL composites

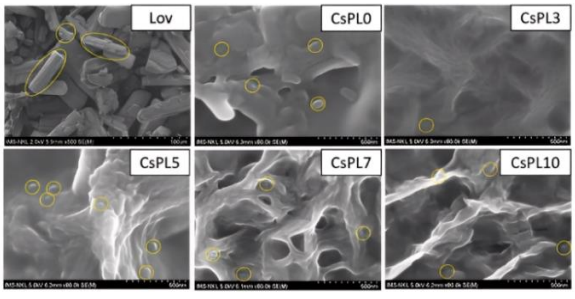

Figure 4. FESEM images of CsPL composites with variable PANi contents

FESEM analysis (Figure 4) demonstrates the profound impact of the Cs/PANi matrix on lovastatin morphology. Pure Lov consists of large, irregular rod-like crystals (10 - 60 μm) [6], while within the CsPL composites, Lov particles are significantly smaller (0.05-0.2 μm) and uniformly dispersed. This size reduction and enhanced dispersion are driven by hydrogen bonding between chitosan's -NH_2 groups and Lov's -OH groups, which promotes integration into the composite's 3D network, inhibiting aggregation [19].

The PANi content critically governs dispersion efficiency. The CsPL7 formulation achieved optimal performance, with spherical Lov particles of 0.05 - 0.08 µm exhibiting excellent dispersion. At lower PANi ratios (CsPL3, CsPL5), an underdeveloped PANi network provided insufficient anchoring sites, leading to free drug diffusion and larger, irregular particles. Conversely, at a higher PANi content (CsPL10), excessive aggregation of hydrophobic PANi chains created domains that promoted uncontrolled Lov crystallization and increased particle size. The CsPL7 ratio thus represents an optimal balance, maximizing the synergistic interaction between Cs and PANi to create a homogeneous matrix for uniform drug dispersion [20]-[21].

2.2.3. Thermal properties of the lovastatin-loaded composites

2.2.3.1. Thermal properties of CsL composites

The DSC analysis (Figure 5) and corresponding thermal parameters (Table 3) demonstrate a significant melting point depression of lovastatin within the CsL composites. Pure Lov melts at 174.6 °C, while the composites exhibit a second, lower melting endotherm. This depression is attributed to reduced drug crystallinity and particle size from dispersion in the chitosan matrix, and hydrogen bonding between Lov and the polymer backbone [22]. The CsL7 and CsL10 samples showed the lowest melting points (~58.3 °C), indicating optimal dispersion. Higher drug loading led to particle aggregation, increasing the melting point relative to these optimal samples, though it remained below pure Lov. This thermal behavior aligns with SEM data, confirming the morphology-dispersion relationship. The observed melting point depression suggests these systems have strong potential for rapid and controlled drug release.

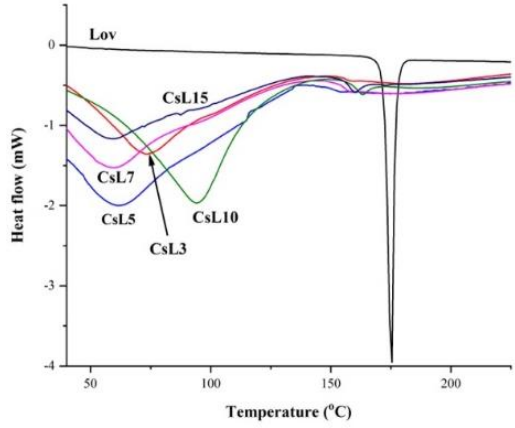

Figure 5. DSC diagrams of Lov and CsL composites with variable Lov contents

Table 3. DSC parameters obtained with Lov and CsL composites

Samples	1st endothermic peak (°C)	2nd endothermic peak (°C)
Lov	-	174.61
CsL3	75.0	158.33
CsL5	62.5	141.67
CsL7	58.33	158.30
CsL10	58.35	158.33
CsL15	93.75	162.57

2.2.3.2. Thermal properties of CsPL composites

The DSC analysis (Figure 6) and corresponding thermal parameters (Table 4) confirm the altered thermal behavior of lovastatin within the CsPL composites. Pure Lov exhibits a single melting endotherm at 174.6 °C, while the composites display two events: polymer matrix dehydration and a significantly depressed Lov melting peak. This melting point depression indicates the drug is stabilized in an amorphous state upon dispersion within the polymer network [21]. The CsPL7 sample showed the most substantial melting point reduction (133.33 °C), signifying the highest degree of amorphization. This superior dispersion is attributed to the effective interaction of PANi within the chitosan matrix, which enhances the composite's structural properties [6]. The excellent correlation between this thermal data and prior SEM results, where CsPL7 exhibited the smallest, most uniform particles, robustly confirms the successful formation of a homogeneous composite with optimal drug integration. This amorphous state is highly favorable for enhancing drug release performance.

Table 4. DSC parameters obtained with Lov and CsPL composites

Samples	1st endothermic peak (°C)	2nd endothermic peak (°C)
Lov	-	174.61
CsPL0	58.35	158.33
CsPL3	99.98	160.01
CsPL5	100.13	161.02
CsPL7	75.02	133.33
CsPL10	133.33	168.75

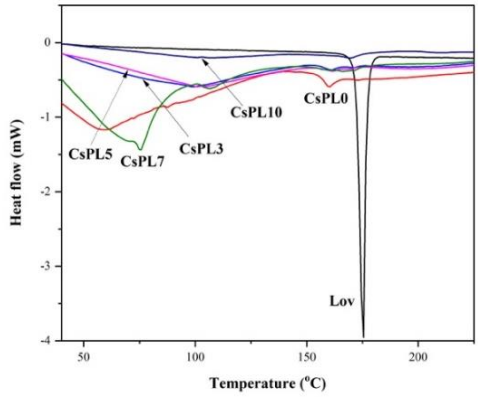

Figure 6. DSC diagrams of Lov and CsPL composites with variable PANi contents

2.2.4. Lovastatin release from composites

**** Lovastatin release from CsL composites***

The drug release profiles of CsL composites (Figure 7) exhibited a biphasic mechanism: an initial burst release from surface-localized lovastatin, followed by a sustained phase governed by matrix swelling and diffusion of internally entrapped drug [14]. A strong pH-dependent release was observed. In simulated gastric fluid (pH 2.0), cumulative release after 30 hours was low (8.81–16.15%), with CsL3 showing the highest and CsL7 the lowest release. Conversely, in simulated intestinal fluid (pH 7.4), release

was significantly enhanced due to chitosan swelling, with the CsL10 sample demonstrating an optimal profile of 96.50% release. This pH-responsiveness is ideal for protecting the drug in the stomach and ensuring efficient intestinal absorption. The drug loading level critically influenced the release efficiency. At low loadings (e.g., CsL3, CsL5), the high percentage release corresponded to a low absolute drug amount, potentially yielding subtherapeutic doses. At excessively high loading (CsL15), drug crystallization and pore saturation occurred, leading to an initial burst followed by incomplete release of trapped internal drug due to hindered diffusion [6]. The CsL10 sample represented the optimal threshold, where the drug load was compatible with the matrix's encapsulation capacity, enabling uniform distribution and controlled, efficient diffusion. These release kinetics are fully consistent with the thermal (DSC) and morphological (SEM) data, which indicate optimal dispersion and amorphous character for the CsL10 formulation.

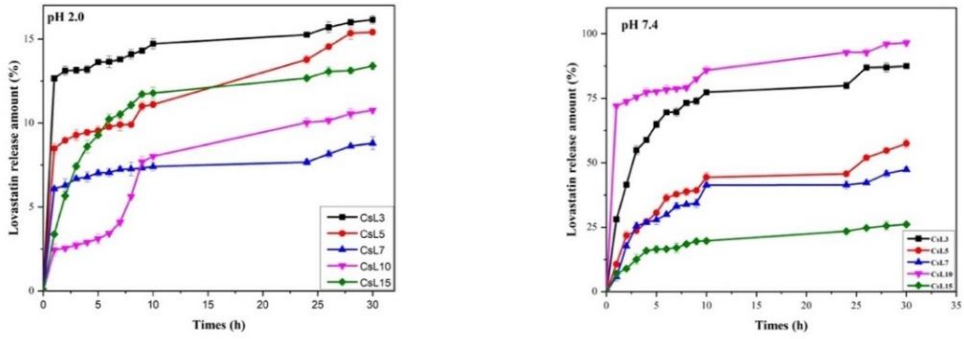

Figure 7. Plots of time-dependent Lov amounts released from CsL composites at pH 2.0 and pH 7.4

**** Lovastatin release from CsPL composites***

The in vitro release of lovastatin from CsPL composites (Figure 8) exhibited a biphasic mechanism: an initial burst from surface drug, followed by sustained release governed by matrix swelling and diffusion of internally entrapped drug [14]. A pronounced pH-dependent release was observed. In simulated gastric fluid (pH 2.0), cumulative release after 30 hours was moderate (10.75 - 29.21%). Conversely, in simulated intestinal fluid (pH 7.4), release was significantly enhanced (76.21 - 98.99%) due to matrix swelling, with CsPL7 demonstrating an optimal profile (95.84% release). This pH-responsiveness is ideal for gastro-protection and maximizing intestinal bioavailability. The PANi content critically governed the release kinetics. At low PANi ratios (3%, 5%), the underdeveloped composite network resulted in high porosity and weak drug-matrix interactions, causing an initial burst release and poor sustained control. Conversely, at a high PANi loading (10%), PANi chain aggregation created dense, hydrophobic regions that clogged diffusion pathways, leading to slow and incomplete release of trapped drug [11]. The 7% PANi ratio (CsPL7) represented an optimal balance, creating a homogeneous microstructure that effectively modulated the release kinetics through controlled physical and chemical interactions. This optimal formulation not only prevented excessive burst release but also ensured efficient and nearly complete drug release in the intestinal environment, maximizing therapeutic potential.

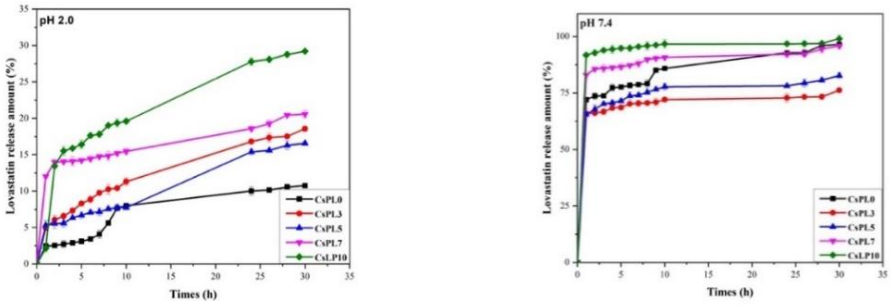

Figure 8. Plots of time-dependent Lov amounts released from CsPL composites at pH 2.0 and pH 7.4

3. Conclusions

A multifunctional chitosan/polyaniline/lovastatin (CsPL) system was developed based on the optimized CsL10 composite. The conductive PANi enabled controlled drug release alongside potential bioelectronic applications. The CsPL7 formulation demonstrated optimal pH-responsive kinetics, with minimal gastric release (20.57%, pH 2.0) and high intestinal release (95.84%, pH 7.4). PANi integration effectively modulated the polymer matrix, establishing CsPL as a promising platform for advanced therapeutic and bioelectronic applications.

REFERENCES

[1] Henwood JM & Heel RC, (1988). Lov: a preliminary review of its pharmacodynamic properties and therapeutic use in hyperlipidaemia. *Drugs* 36(4), 429-454.

[2] Chandrasekaran M, Kim KD & Chun SC, (2020). Antibacterial activity of chitosan nanoparticles: A review. *Processes,* 8(9), 1173.

[3] Alberts AW, (1990). Lov and simvastatin-inhibitors of HMG CoA reductase and cholesterol biosynthesis. *Cardiology*, 77(Suppl 4), 14-21. Doi: 10.1159/000174688

[4] Nguyen NL, Vu QM, La CG, Nguyen TC, Hoang TD, Tran TTD, Thai H & Vu QT, (2024). Assessment of the hemostatic ability of biomaterial based on chitosan and *Eclipta prostrata* L. extract. *Biomedical Materials*, 19(3), 035026.

[5] Dam XT, Duong TM, Mai DH, Thai H, Vu VA, Vu QT, Ngo TCQ, Nguyen TA & Nguyen TC, (2024). Preparation of the novel bio-nanocomposites based on chitosan, *Piper betle* leaf extract, and MgO nanoparticles for chili preservation. *Polymer Engineering & Science,* 64(6), 2795-2811.

[6] Ha MH, Vu QM, Vu TTT, Dao TPT, Pham TD, Nguyen TBV, Duong KL, Nguyen NL, Doan TYO, Nguyen TC, Thai H & Vu QT, (2022). Evaluation of the effect of the chitosan/carrageenan ratio on Lov release from chitosan/carrageenan based biomaterials. *Vietnam Journal of Chemistry*, 60(S1), 72-78.

[7] Karimi M, Ghasemi A, Zangabad PS, Rahighi R, Basri SMM, Mirshekari H & Hamblin, (2016). pH-Responsive polymers: Synthesis, properties, and applications in drug delivery. *Advanced Drug Delivery Reviews*, 107, 1-26.

[8] Zhang Y, Zhou M, Dou C, Ma G, Wang Y, Feng N, Wang W & Fang L, (2019).

Synthesis and biocompatibility assessment of polyaniline nanomaterials. *Journal of Bioactive and Compatible Polymers,* 34(1), 16-24.

[9] Pramanik N, Dutta K, Basu RK & Kundu PP, (2016). Aromatic π-conjugated curcumin on surface-modified polyaniline/polyhydroxy alkanoate-based 3D porous scaffolds for tissue engineering applications. *ACS Biomaterials Science & Engineering*, 2(12), 2365-2377.

[10] Fan Q, Sirkar KK & Michniak B, (2008). Iontophoretic transdermal drug delivery system using a conducting polymeric membrane. *Journal of Membrane Science*, 321(2), 240-249.

[11] Zhang L, Zhang Z, Kilmartin PA & Travas-Sejdic J, (2011). Hollow polyaniline and indomethacin composite microspheres for controlled indomethacin release. *Macromolecular Chemistry and Physics*, 212, 2674-2684.

[12] Shokry H, Vanamo U, Wiltschka O, Niinimäki J, Lerche M, Levon K, Linden M & Sahlgren C, (2015). Mesoporous silica particle-PLA–PANI hybrid scaffolds for cell-directed intracellular drug delivery and tissue vascularization. *Nanoscale*, 7, 14434-14443.

[13] Yang YF, Meng FY, Li XH, Wu NN, Deng YH, Wei LY & Zeng XP, (2019). Magnetic graphene oxide-Fe_3O_4-PANI nanoparticle adsorbed platinum drugs as drug delivery systems for cancer therapy. *Journal of Nanoscience and Nanotechnology*, 19(12), 7517-7525.

[14] Minisy IM, Salahuddin NA & Ayad MM, (2021). In vitro release study of ketoprofen loaded chitosan/polyaniline nanofibers. *Polymer Bulletin*, 78, 5609-5622.

[15] Ghorbani F & et al., (2022). A smart magnetic chitosan/agarose/halloysite nanotube hydrogel for sustained release of doxorubicin. *International Journal of Biological Macromolecules*, 219, 216-227.

[16] Webber V, Carvalho SM, Ogliari PJ, Hayashi L & Barreto PLM, (2012). Optimization of the extraction of carrageenan from *Kappaphycus alvarezii* using response surface methodology. *Food Science and Technology*, 32(4), 812-818.

[17] Sirotkin N & Khlyustova A, (2023). Plasma synthesis and characterization of PANI + WO_3 nanocomposites and their supercapacitor applications. *Journal of Composites Science*, 7(4), 174.

[18] Drabczyk A, Kudłacik-Kramarczyk S, Głąb M, Kędzierska M, Jaromin A, Mierzwiński D & Tyliszczak B, (2020). Physicochemical Investigations of Chitosan-Based Hydrogels Containing Aloe Vera Designed for Biomedical Use. *Materials*, 13, 3073.

[19] Jamil B, Habib H, Abbasi S, Nasir H, Rahman A, Rehman A & Imran M, (2016). Cefazolin-loaded chitosan nanoparticles to cure multidrug-resistant Gram-negative pathogens. *Carbohydrate Polymers*, 136, 682-691.

[20] Bhadra J & Sarkar D, (2019). Effect of dopant type on the properties of polyaniline-based nanocomposites. *Polymer Bulletin*, 76(8), 4275-4289.

[21] Luo Y, Liu J, Zeng J & Pan H, (2024). Global burden of cardiovascular diseases attributed to low physical activity: An analysis of 204 countries and territories between 1990 and 2019. *American Journal of Preventive Cardiology,* 17, 100633.

[22] Loc TT, Thai H, Nguyen TC & Le DG, (2018). The effects of the compatibilizers on the lovastatin release form the alginat/chitosan/Lov composite. *Vietnam Journal of Chemistry*, 56(3), 389-395 (in Vietnamese).